[Article ID] 1003- 6326(2001) 04- 0529- 06

Structure of nanocrystalline WC-10% Co powder[®]

YANG Zhi min(杨志民)¹, MAO Chang hui(毛昌辉)¹, DU Jun(杜 军)¹, Michel Daniel², Champion Yannick², Hagège Serge², Hytch Martin² (1. General Research Institute for Nonferrous Metals, Beijing 100088, P. R. China; 2. Centre d'Etudes de Chimie Métallurgique/CNRS, 94407 Vitry-sur-Seine, France)

[Abstract] Nanostructured WC-Co powders obtained by mechanical milling were investigated by combination of X-ray diffraction (XRD) and high resolution transmission electron microscopy (HRTEM) techniques. Rietveld analysis indicates that the experimental XRD patterns cannot be satisfactorily explained with the hexagonal WC structure. HRTEM image analysis shows that in the as milled nanostructured powder, many WC grains contain stacking faults lying on the plane $\{10 \cdot 0\}$. Analysis of phase images show that these defects are nearly periodically ordered along the $[10 \cdot 0]$ direction. Based on these observations, a structural model was proposed for the WC grains with ordered stacking faults, which is in fact equivalent to a superstructure of WC with space group Amm2. When this model describing the faulted fraction of WC is introduced together with the normal WC structure (space group $P\bar{6}m2$) into the Rietveld refinement, a much better a greement between the calculated and experimental XRD profiles was obtained. This study allows to obtain the lattice parameters, grain size, microstrain and other structural information on the as milled powders.

[Key words] structural properties; mechanical milling; WC-Co

[CLC number] TG 115. 221. 3

[Document code] A

1 INTRODUCTION

Nanocrystalline materials exhibit a crystallite size in the range of a few nanometers (typically 5~ 20 nm), such that a significant fraction of the material is near incoherent interfaces between crystals of different orientation. Hence nanocrystalline materials are expected to have different properties from both crystalline and amorphous materials. It was reported that the mechanical properties of nanocrystalline WC-10% Co cemented carbides are much better than conventional materials [1~3]. A lot of processes have been investigated for synthesizing nanocrystalline materials. Among them, high-energy mechanical milling was widely adopted because of its low cost, efficiency and simplicity of processing.

In previous studies^[4,5], nanocrystalline WC-10% Co powder mixtures were prepared by high-energy ball milling and studied by XRD and HRTEM. The lattice parameters, size and strain were analyzed by line profile analysis using the Halder-Wagner plot^[6]. Recently, another study by Ungar et al^[7] allowed to determine the particle size, the size distribution and dislocation density in a nanocrystalline tungsten carbide using a modified Williamsom-Hall and Warrem-Averbach method. A log-normal size distribution was obtained for particle size and a high dislocation density was found for the ball-milled powder. The dislocation density decreases by about two orders of magnitude after annealing.

In both previously mentioned studies, peaks were fitted separately and the information on relative intensities of each peak was not considered. Another problem comes for WC from the overlapping of XRD peaks, especially at high diffraction angle, due to the severe broadening met in nanocrystalline samples. This limits accurate profile studies to well separated peaks. Whole pattern fitting developed recently by Langford et al^[8] for studying the effect of a crystallite size distribution allows to overcome the overlapping problem and to take into account the line intensities.

In this work, we tried a Rietveld (whole profile) analysis for the refinement of the experimental XRD patterns. The Rietveld method has the advantage of performing a whole pattern fitting taking into account intensities and overlapping. It rapidly appears that the XRD whole profiles could not be satisfactorily fitted using only the modeled whole pattern of WC including line broadening. In fact, intensity residues, either by excess or defect, were systematically found close to the Bragg positions. These discrepancies between calculated and observed intensities indicate that the WC structure introduced in the refinement cannot correctly represent the crystal structure of the material and that significant structural modification has been induced by the milling process.

Actually, HRTEM observations revealed that many nanocrystallites are heavily affected by stacking faults^[4]. We have analyzed these defects; they are not randomly dispersed, but are organized with a

Tereived date 2000 - 08 - 18; [Accepted date] 2001 - 01 - 17

nearly regular periodicity. This study reports on a model introducing a WC superstructure including stacking faults for explaining HRTEM observations and XRD patterns.

2 EXPERIMENTAL

Samples of different milling time were prepared using a Spex-8000 three dimension vibrating high-energy ball mill. The milling vial and milling balls are made of WC-Co in order to avoid an eventual contamination. The mass ratio of milling balls to powder mixture was fixed to 8:1. The milling times were 0.5, 1, 2, 5, 10, 20, 40, 100, 150 h respectively.

The XRD patterns were taken using a Philips Xray diffractometer with CoK_{α} radiation. In order to ensure a good counting statistics, data were collected with a step of 0.02° and counting time of 15s for each step. Rietveld (whole profile) analysis of the experimental XRD patterns were carried out using the Fullprof software and Rietveld refinement guidelines^[9,10]. A polynomial function was used to extract the background from the patterns; a well-crystallized LaB₆ standard was used to get the instrument resolution function; a Thompson-Cox-Hastings function was selected as the peak shape function. The quality of agreement between the experimental and calculated profiles is seen from the difference curve, but is also measured by the profile R_p and the weighted profile $R_{\rm wp}$:

$$R_{\rm p} = 100 \sum_{i=1}^{\infty} Y_{i\rm exp} - Y_{i\rm cal} / \sum_{i=1}^{\infty} Y_{i\rm exp} / X_{i\rm exp}$$

$$R_{\rm wp} = 100 \sum_{i=1}^{\infty} W_{i} (Y_{i\rm exp} - Y_{i\rm cal})^{2} / X_{i\rm exp} / X_{i\rm exp}^{2}$$

HRTEM observation was carried out using a 200 kV TOPCON-002B ultra high resolution analytical electron microscope.

3 RESULTS

The XRD pattern of a WC-10% Co composite powder before milling is shown in Fig. 1. The perfect crystal structures for hexagonal tungsten carbide (space group $P\bar{6}m2$) and cubic cobalt (space group Fm3m) were used for the Rietveld refinement. The difference curve shows that the calculated pattern is in good agreement with the experimental pattern, indicating that there are few structural defects in the starting powder. From this figure it also can be seen that the reflection peaks of Co are very weak.

Fig. 2 shows the XRD pattern of the powder milled for 10h. Strong broadening and overlapping can be seen compared with the sample without milling. Actually after 2h milling, the peaks of Co get broad enough to submerge in the background and can not be observed in the experimental condition. So

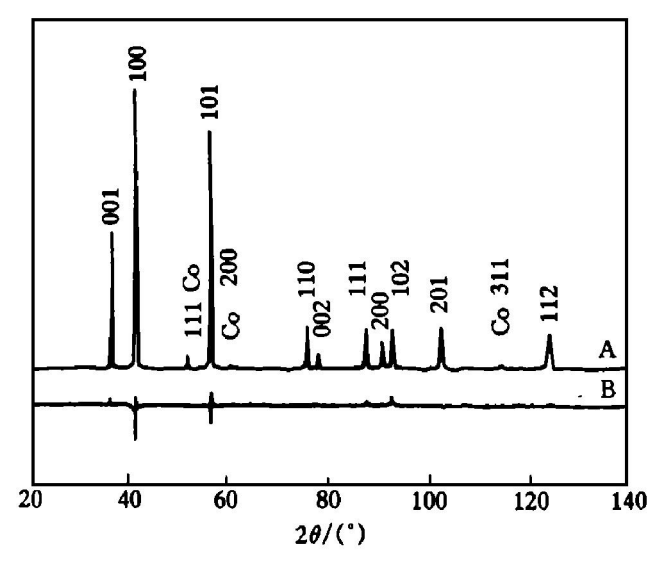


Fig. 1 XRD patterns of starting WC-Co powder A—Experimental pattern;
B—Difference curve (experimental—calculated)

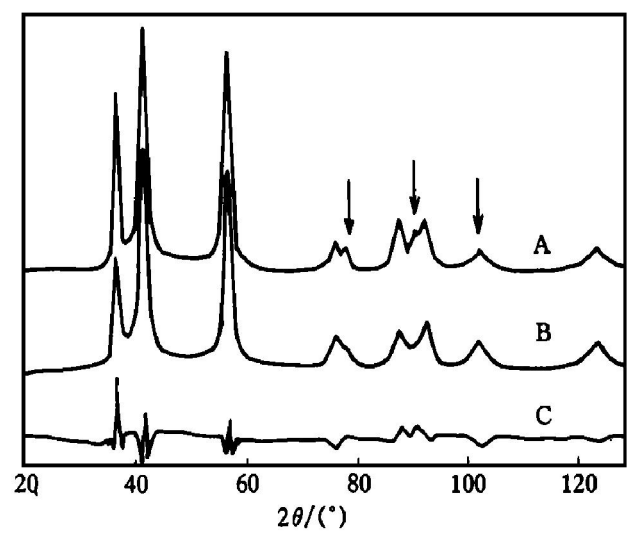


Fig. 2 XRD experimental pattern and fitting result when WC structure was used for powder milled for 10 h A—Experimental pattern; B—Calculated pattern; C—Difference curve

only WC was used to fit the experimental patterns of the as milled powders in the following analysis. When the perfect structural model was used to refine the experimental pattern, we find that there are systematic differences between the calculated pattern and the experimental pattern for all the as milled specimens.

First, the relative intensities of some peaks change compared with the pattern of the starting powder. The experimental intensities of peak (20°0) and peak (00°2) are much stronger than the calculated ones, as shown by the difference curve in Fig. 2. This phenomenon can not be caused by preferred orientation effect, because the relative intensities of peak (10°0) and peak (20°0) have to be interrelate and in this case, the $I_{\rm cal}$ (20°0) (integrated intensity) is only 70% of $I_{\rm exp}$ (20°0), while $I_{\rm cal}$ (10°0) is nearly

98% of $I_{\text{exp}}(10^{\bullet}0)$.

Second, not all the peak profiles can be well described. For example, it was not possible to match well the peak (20•1) in the whole profile matching process, even if anisotropic strain and domain size effects were taken into account.

It was thus likely that these phenomena might be caused by structural defects created during mechanical milling. From the HRTEM study at atomic scale, it appeared that two types of WC nanocrystals were found. In particular, in addition to crystallites containing few defects, the smaller grains contained a large number of planar defects. Fig. 3(a) shows the HREM images of such an as milled WC grain. The defects correspond to the stacking fault {10•0} 1/6[12•3], which is the most typical type of stacking faults found in WC crystals^[11]. Besides, these stacking faults are periodically arranged within the nanograin. This periodicity can be visualized using the phase analysis method developed by Hÿtch^[12]. In

Fig. 3(b), the power spectrum of the image is shown where two sets of periodicity associated to plane $\{00^{\bullet}1\}$ and plane $\{10^{\bullet}0\}$ can be seen. Figs. 3(c) and (d) are phase images P $10^{\bullet}0$ (r) and P $00^{\bullet}1$ (r) reconstructed by inverse Fourier using the two reflections $10^{\bullet}0$ and $00^{\bullet}1$ in Fig. 3(b). The phase image $P_g(r)$ can be used to define the translation domain associated to a given diffraction vector \mathbf{g} within a crystal grain. The phase shift is represented on a grey scale. In particular, when the fringe shifts by half a period, the phase changes by π , resulting in the different color at both sides of the interface; on the other hand, when the fringe does not shift or shifts by a period, the phase is kept constant and the color is the same across the field of view.

The phase image P $10 \cdot 0(r)$ (Fig. 3(c)) shows almost the same color across the whole WC particle. From Fig. 3(d), it can be seen that the WC grain has several parts of different colors, each corresponds to a stacking fault. It is important to notice that in the

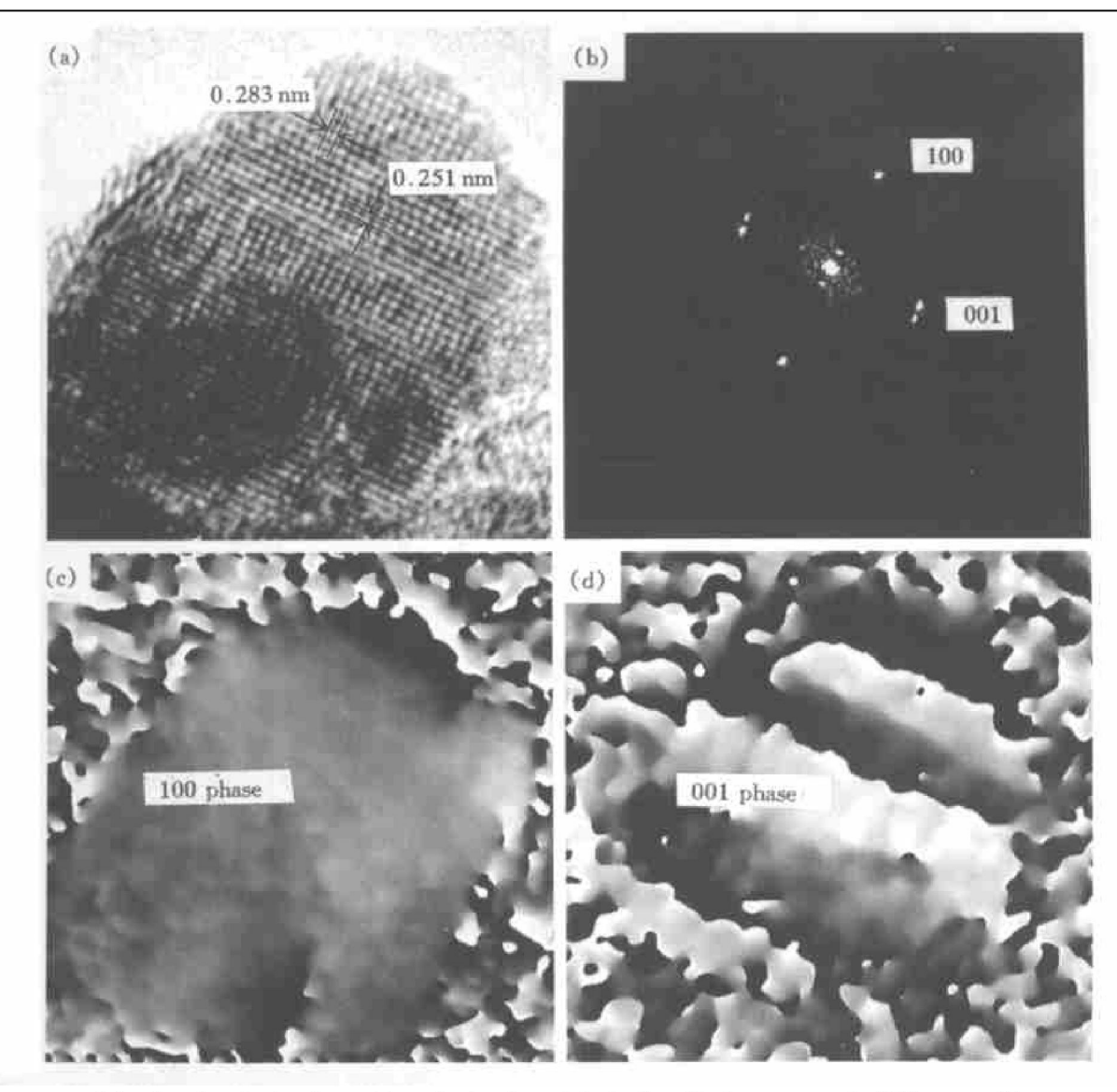


Fig. 3 Analysis of stacking faults found in ball-milled nanometric WC crystallites (a) —HRTEM image; (b) —Diffraction of image; (c) —Phase image P10•0(r); (d) —Phase image P00•1(r)

diffraction pattern (Fig. 3(b)), the defects suppress the 00°1 spot which is replaced by a pair of satellite spots. The distance in reciprocal space between these two satellites is directly related to the periodicity or pseudoperiodicity of the stacking defect. Consequently, in the XRD patterns, the presence of the observed stacking defects will reduce the intensity of given lines such as 00°1 and introduce extra intensity out of Bragg positions at the angle corresponding to the satellite spots.

4 DISCUSSION

A tentative structure model for the faulted WC grains is proposed for representing an ordered array of stacking faults. According to this model, the faulted structure of hexagonal WC can be described by a structure with space group Amm2, in which there is one stacking fault every a certain number (defined as a variable "n") of planes {10•0}. The number "n" can be adjusted in order to correspond to the satellite positions. Fig. 4 represents a structure model with one stacking fault every 7 planes.

The as milled powder will be now considered a mixture of WC grains of two different structures: $P\bar{6}m2$ and Amm2. These two phases were then put into the Rietveld refinement process. In this case, the XRD experimental patterns can be fitted much better, as shown by the difference curve in Fig. 5 which corresponds to a sample obtained after a milling time of 10 h. The improved agreement between the experimental and calculated profiles was also measured by the factors R_p and R_{wp} which decreased by about 50 percent. The previously mentioned intensity deficiencies, for instance concerning the peak (20•0), are

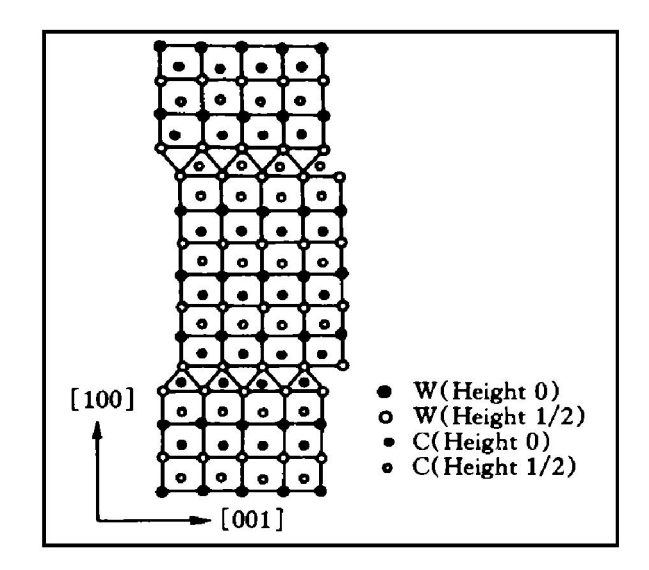
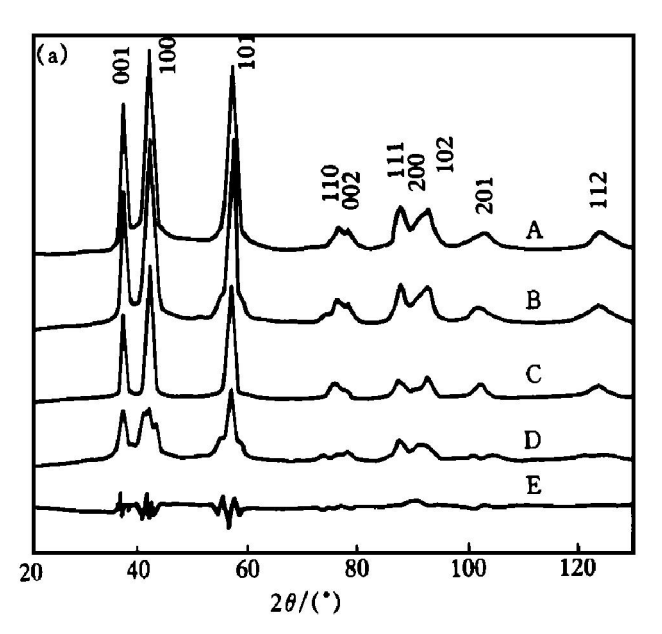


Fig. 4 Structure model for faulted hexagonal WC (Space group Amm2)

corrected by the introduction of stacking faults. For the WC grains with stacking faults, the WC peak (20•1) is split into two peaks in the orthorhombic phase and this allows the experimental peak shape to be fitted by adding the intensities of the two parts, as shown in Fig. 5(b). This could not be made using only the WC structure. So it can be concluded that the stacking faults are the cause of the differences observed from a XRD pattern of WC solely broadened by size and strain effects. A reasonably good fit was obtained for all samples with different milling time. The superstructure used assumes a perfectly regular spacing of the stacking fault, it is likely that a even better adjustment of the calculated patterns to the experimental ones could be achieved if some fluctuation of stacking fault distances was permitted in associa-



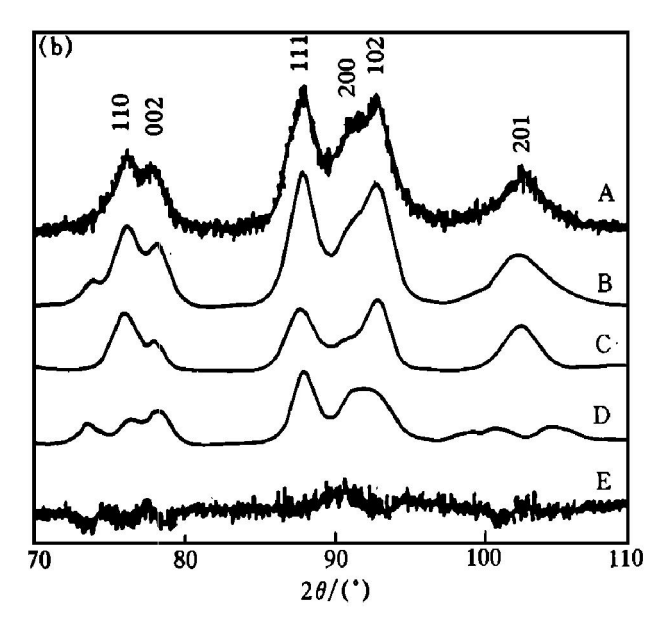


Fig. 5 XRD pattern of specimen milled for 10 h and the fitting results when stacking faults are taken into account in the refinement (Fig. 5(b) is a zoom)

A Experimental pattern; B Calculated pattern (C+ D); C Calculated pattern for the hexagonal phase with stacking faults;

D Calculated pattern of the part without stacking faults; E Difference curve (A-B)

tion with the distribution in particle size observed by TEM. From the refinements made on all the samples, we get strain, grain size, lattice parameters and information on the stacking fault periodicity. Results reported in Table 1 show that the volume fraction of the faulted WC grains is nearly 50% for many samples. The plane number between stacking faults decreases rapidly from 17 to 9 in the first five hours. As the milling time increases, the amount of stacking faults does not change noticeably. It is shown that in our milling conditions, the preferred mode of deformation is the formation of a large number of stacking faults which tend to be ordered in smaller grains. This ordering seems to be destabilized by prolonged milling during 150h. We do not know whether cobalt, which was mainly found by EDX analysis in TEM along WC grain boundary regions, may affect these phenomena.

Table 1 Volume fraction of hexagonal WC and orthorhombic WC defective superstructure (n is number of (10•0) planes between defects,

D is spacing between defects)					
Milling	Volume fraction		$R_{\rm p}$	n	D
time/ h	Hexagonal	Orthorhombic			/ nm
150	0.72	0.28	4.97	7	1.8
100	0. 52	0.48	6.67	9	2.3
40	0.41	0.59	6.05	9	2.3
20	0.38	0.62	5.59	9	2.3
10	0.46	0.54	7.49	9	2.3
5	0. 47	0.53	6.46	9	2.3
2	0.43	0.57	7.47	11	2.8
0. 5	0. 47	0. 53	6.73	17	4. 3

Fig. 6 shows the variation of the unit cell volume $(2\cos 60^{\circ} \cdot A^{2} \cdot C, A \text{ and } C \text{ are cell parameters})$ for the phase corresponding to hexagonal WC grains in

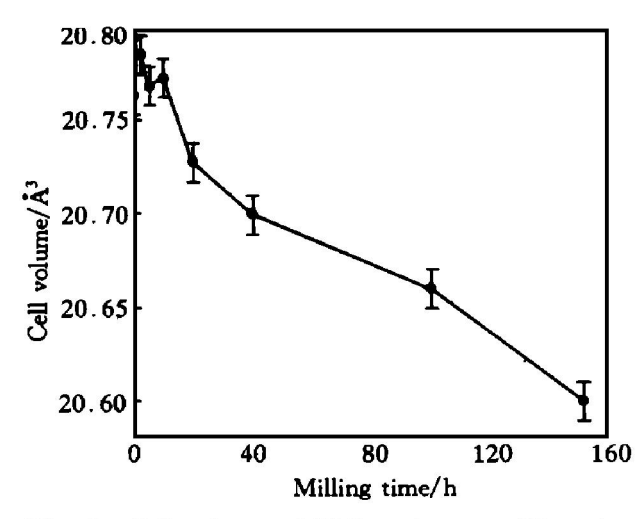


Fig. 6 Cell volume of WC grains vs milling time

function of the milling time. Both A and C decrease as the milling time increases. It can be seen that the unit cell volume decreases slightly with the milling time. This effect can be induced either by mechanical effects and the presence of defects or by chemical modification if some cobalt can be dissolved in the crystallites.

The hexagonal WC grain size decreases rapidly in the first stages of milling, while after 10 h of milling it decreases much more slowly (Fig. 7). In agreement with TEM observations, the crystallite dimensions are relatively isotropic. On the other hand, the lattice strain found for hexagonal WC crystallites shows a strong anisotropy. The lattice strain along [10•0] in the powder milled for 10 h is much higher than along [00•1] (Fig. 8). This result is also probably due to the planar defects which, despite they are less numerous than in the so-called orthorhombic crystallites, are also found in hexagonal WC grains.

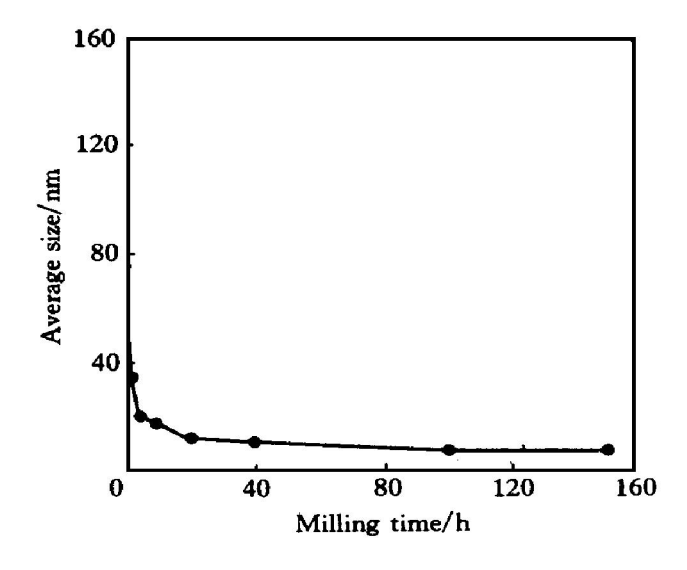


Fig. 7 Grain size of WC vs milling time

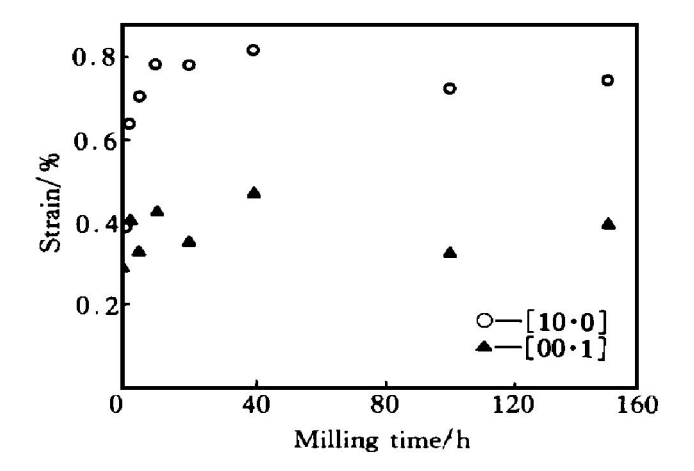


Fig. 8 Strain along [00•1] and [10•0] vs milling time for WC-10% Co powder

5 CONCLUSIONS

1) For the mechanically milled WC-10% Co

powder, the relative intensities of some peaks of XRD patterns are modified as compared with those before milling, and the profiles can not be described when the hexagonal structure model for the WC grains is only used in the Rietveld analysis process.

- 2) HRTEM images show that stacking faults in the planes {10•0} of WC grains are created by milling. Based on the HRTEM observations revealing the regular array of these defects in many crystallites, a structure model was proposed for the WC grains with stacking faults. When this new "phase" is put into the Rietveld procedure, the quality of the refinement is much improved. The refinement results show that during mechanical milling the density of stacking faults increases quickly during the first five hours, and as the milling time increases it stays almost unchanged.
- 3) During mechanical milling, the cell volume of the WC decreases slowly. The average grain size decreases rapidly at the first 5 h and then decreases slowly to about 8 nm. Microstrain along [10 0] is much larger than along [00 1] for the milled samples.

[REFERENCES]

- [1] Ettmayer P. Properties of nano crystalline materials [J]. Annals of Materials Science, 1989, 19: 145.
- [2] Suryanarayana C. Nano crystalline materials [J]. International Materials Reviews, 1995, 40: 41–50.

- [3] Eckert J, Holzer J C, Krill III C E, et al. Structural and thermodynamic properties of nano-crystalline fcc metals prepared by mechanical attrition [J]. J Mater Res, 1992, 7: 1751-1758.
- [4] Mao C H, Du J, Champion Y, et al. Study on nanostructured WC-Co composite powders made by mechanical milling [J]. Rare Metals, 1998, 4: 241-245.
- [5] Mao C H, Du J, Champion Y, et al. Mechanical alloying of WC Co [A]. 6th Conference and Exhibition of the European Ceramic Society, British Ceramic Proceedings n° 60 vol. 1 [C]. Brighton, 1999. 399–401.
- [6] Langford J I. Accuracy in Powder Diffraction II [M]. NIST Special Publication N° 846. 1992. 110–115.
- [7] Ungar T, Borbély A, Gorerr Muginstein G R, et al. Solgel processing of electrical and magnetic ceramics [J]. Nano structured Materials, 1999, 11: 103.
- [8] Langford J I, Louër D, Scardi P. Effect of a crystallite size distribution on X-ray diffraction line profiles and whole powder pattern fitting [J]. J Appl Crystal, 2000, 33: 964-970.
- [9] Rodriguez Carvajal J. Reference Guide for the Computer Program Fullprof [M]. Laboratoire Léon Brillouin, CEA-CNRS, Saclay (France). 1998. 1-73.
- [10] McCusker L B, Von Dreele R B, Cox D E, et al. Rietveld refinement guidelines [J]. J Appl Crystal, 1999, 32: 36-50.
- [11] Hagège S. Analysis of the Dislocations of Tungsten Carbide, (in French), [D]. University of Caen, 1980. 14
 33.
- [12] Hytch M J, Potez L. Geometrical phase analysis of high-resolution electron microscopy images of antiphase domains example Cu₃Au [J]. Phil Mag A, 1997, 76: 1119-1152.

(Edited by YUAN Sai-qian)